



Synthesis, characterization and catalytic performance of titania supported VPO catalysts for the ammoxidation of 3-picoline

V.N. Kalevaru*, N. Madaan, A. Martin

Leibniz-Institut für Katalyse e.V. an der Universität Rostock, Albert-Einstein-Str. 29a, D-18059 Rostock, Germany

ARTICLE INFO

Article history:

Received 26 February 2010

Received in revised form 17 June 2010

Accepted 19 July 2010

Dedicated to 75th birth anniversary of Prof. Dr. H. Knözinger, University of Munich, Germany.

Keywords:

Ammoxidation

3-Picoline

Nicotinonitrile

VPO catalysts

Acidity characteristics

ABSTRACT

Series of vanadium phosphorus oxide (VPO) catalysts supported over titania (anatase) were synthesised with varying contents of VPO (5–50 wt%). These solids were characterised by ICP-OES, TG/DTA, BET, XRD, FTIR (Py-ads) and XPS. The catalytic activity was evaluated for ammoxidation of 3-picoline (3-pic) to nicotinonitrile (NN) in a fixed bed catalytic reactor. Thermal analysis provided good hints on the phase transformation of VHP precursor into active VPP phase at around 400 °C. BET surface areas and pore volumes are found to depend on VPO loading and varied in the range from 70 m²/g to 133 m²/g. XRD demonstrates the formation of (VO)₂P₂O₇ (VPP) phase. XPS showed that an average oxidation state of vanadium around 4.0, which is found to be unaltered in the spent samples. FTIR (Py-ads) revealed the presence of both Lewis and Brønsted sites with varying proportions, which again depend upon VPO loading. Correlation of acidic properties (Lewis and Brønsted acid sites) of the catalysts with that of performance of catalysts was explored. VPO loading has a clear influence on the acidic properties and thereby catalytic activity and selectivity. Catalytic results showed that the supported catalysts gave better performance compared to bulk VPO. Yield of NN increased up to 20 wt% VPO loading and then decreased with further increase in VPO content. Among all catalysts tested, the 20 wt% VPO/TiO₂ exhibited the best performance (X-3-pic = ca. 100% and Y-NN = 83%).

© 2010 Elsevier B.V. All rights reserved.

1. Introduction

Ammoxidation refers to the formation of nitriles by partial oxidation of hydrocarbons in the presence of ammonia [1]. Ammoxidation of substituted aromatics/hetero aromatics opens the way for the direct synthesis of fine chemicals and/or intermediates for fine chemical syntheses [2,3]. Various pharmaceuticals, pesticides, dyestuffs and other speciality products are produced from substituted aromatic or heteroaromatic nitriles [e.g. [4]]. Ammoxidation of alkyl pyridines is one such good example for producing industrially important nitriles. Interestingly, the conversion of methyl pyridines to their corresponding nitriles is relatively easier, economic as well as eco-friendly process. Particularly, the ammoxidation of 3-methylpyridine or 3-picoline (3-pic) to nicotinonitrile (NN) is frequently investigated mainly due to the commercial importance of the nitrile for large-scale production of nicotinamide (niacinamide) and nicotinic acid (niacin/vitamin B3), which are used extensively as feed additives [e.g. [5]]. It is known that human body cannot produce directly either nicotinic acid or nicotinamide on its own and hence it is very much dependent on the intake of these components through foodstuffs. It is also reported elsewhere

[5] that the number of deaths caused by niacin deficiency disease (i.e. pellagra) dropped in the U.S. from 7500 to just 70 in the years from 1929 to 1956. This study clearly shows the importance of niacin in our day to day life.

Even though niacin is found naturally in various foodstuffs (e.g. pork, yeast, wheat etc.), the majority of niacin today is produced synthetically. The worldwide production amounts to 22,000 ton/a in 1995, which is significantly increased to about 35,000–40,000 ton/a in 2006 and the demand is further increasing in recent times [6]. Lonza AG, Switzerland alone produces >15,000 ton of niacin and is the world leader in niacin production. The very classical method (discovered ca. 100 years ago) for the production of niacin was based on oxidation of nicotine using K₂Cr₂O₇. This process is however unattractive today due to significantly larger amounts of waste production (i.e. about 9 ton of waste produced per 1 ton of niacin production). In the direction of change of feedstocks, attempts were also made to use 3-picoline as suitable starting material for the production of niacin by means of liquid phase oxidation with permanganate, chromic acid or nitric acid. These processes also suffer similar problem of larger waste (e.g. permanganate process gives 4 ton of waste while chromic acid gives ca. 2 ton of waste per 1 ton of niacin production) [6]. Another alternative to produce niacin is oxidation or ammoxidation of 2-methyl-5-ethyl pyridine (MEP). Ammoxidation of MEP to NN is being practiced at Lonza AG for the past 40 years [5]. Although this

* Corresponding author. Tel.: +49 381 1281284; fax: +49 381 128151284.
E-mail address: narayana.kalevaru@catalysis.de (V.N. Kalevaru).

raw material is cheaper, the process is not really very attractive from ecological point of view due to less carbon efficiency owing to loss of two carbon atoms as CO₂ during its conversion. On the whole, it is generally agreed that among different methods available for niacin/niacinamide production, the 3-picoline is indeed an ideal feedstock from chemical standpoint and the vapour phase ammoxidation is the most preferred route. Ammoxidation of 3-picoline to NN followed by hydrolysis are at present existing commercial processes, e.g. commercialized by Reilly Industries, U.S. and Lonza AG, Switzerland.

Numerous catalytic systems have been developed and applied for the ammoxidation of alkyl aromatics. Generally, the most active and selective catalyst systems used for different ammoxidation reactions are based on V–Ti–O [7], V–Mo–O [8], V–Sb–O [9], VO_x/Nb₂O₅ [10], VO_x/Al₂O₃ [11], VO_x/ZrO₂ [12], Fe–Sb–O promoted by further transition metals [13] and also some zeolite based catalysts [14] are reported to be active and selective. However, the majority of catalysts employed for different ammoxidation reactions contain vanadium as the key component. Favoured supports are titanium oxide (anatase) [15], zirconium oxide [16], tin oxide [17] mixed supports such as titanium–tin oxide [18]. In recent times, metal fluorides are also used as effective supports for vanadia catalysts [19–21].

Furthermore, polyoxometallates [22] and certain metal oxides such as vanadium phosphorous oxides [e.g. [23]], vanadium oxide combined with antimony oxide [24,25] are also used as effective catalytic systems but they are applied mainly in the form of bulk materials. In most cases, VPOs are used in their bulk form mainly for butane to maleic anhydride reaction [e.g. [26]]. On the other hand, investigations on the synthesis and application of supported VPO catalysts are rare, probably due to the difficulty of their synthesis because of the insoluble nature of VPO precursors in known solvents. Nonetheless, preparation of supported VPOs by means of solid–solid wetting is possible, which seems to be a suitable option. With this background, it is intended to extend such synthesis procedure further to various VPO solids and check its influence on the ammoxidation activity. Thus, the goal of the present investigation is to synthesize, characterize and evaluate the catalytic performance of TiO₂ supported VPO catalysts towards selective ammoxidation of 3-picoline to nicotinonitrile. The objective is also to develop highly active and selective catalysts in the direction of maximizing the yield of nicotinonitrile due its high industrial importance.

2. Experimental

2.1. Catalyst preparation

Preparation of supported VPOs involves two steps. First step deals with the preparation of VPO precursor (VOHPO₄·0.5 H₂O (VHP)) by an organic route, while the 2nd step concerns the preparation of TiO₂ (anatase) supported VPO catalysts using the precursor prepared in the 1st step. The samples were then oven dried and calcined under appropriate conditions to obtain active (VO)₂P₂O₇ phase. The details of the two-step preparation procedure are described below.

Preparation of VPO precursor (1st step): 52.5 g sample of V₂O₅ (UH: 2862; Gesellschaft für Elektrochemie, Nürnberg) was suspended in a mixture of 315 ml of 2-butanol (purity > 99%, Merck) and 210 ml of benzyl alcohol (purity > 99%, Merck) at room temperature. The suspension was stirred continuously under reflux for 3 h, then cooled to room temperature and kept under stirring at room temperature for overnight. Then 63.2 g of 85% o-H₃PO₄ was slowly added, and the solution was again heated and maintained under reflux with constant stirring for another 2 h. The resulting slurry was cooled to room temperature, filtered, and washed with

Table 1

List of different VPO catalysts prepared and used in the ammoxidation of 3-picoline to nicotinonitrile.

S. No.	Catalyst	Denotation
1	Bulk VPO	A
2	5 wt% VPO/TiO ₂	B
3	10 wt% VPO/TiO ₂	C
4	15 wt% VPO/TiO ₂	D
5	20 wt% VPO/TiO ₂	E
6	25 wt% VPO/TiO ₂	F
7	50 wt% VPO/TiO ₂	G
8	TiO ₂	H

ethanol. The solid precursor thus obtained was oven dried at 120 °C for 24 h.

Preparation of TiO₂ supported VPO catalysts (2nd step): Desired amounts of VHP precursor and TiO₂ (anatase) powders were mixed together in a mortar by means of physical mixing for about 15 min, i.e. until the colour of solid mixture was perfectly uniform. Using the same procedure, various catalysts over a wide range of VPO contents were prepared. Finally the catalysts were calcined at 450 °C, 3 h, 1% O₂/N₂. VPO loading was varied from 5 wt% to 50 wt% and the P/V ratio was kept constant at 0.95. The list of catalysts prepared and their denotation is given in Table 1. It should be noted that uncalcined TiO₂ support was used as it is in preparing various catalysts. However, the weight loss of TiO₂ during calcination is considered in calculations and accordingly the weight of TiO₂ is taken. In addition, one should also note that the TiO₂ support obtained is a commercial sample supplied by Kronos, Germany, which is prepared using sulphate precursor and hence this support material contains certain amounts of residual sulphates in it. Removal of such sulphates is also observed during TG/DTA measurements and is also discussed below in a separate section. The detailed procedure for the preparation of these catalysts is described elsewhere [27,28].

2.2. Characterization of catalysts

ICP-OES (Optima 3000XL, Perkin-Elmer) using a microwave pressure digestion (MDS 200; CEM) with hydrofluoric acid and aquaregia at 9 bar was used to analyse the chemical composition of fresh and spent catalysts. All the samples were analysed twice and the results presented here are the average values.

Thermogravimetric analysis (TGA) was carried out using simultaneous TG and DTA instrument (Netzsch GmbH, model: STA 409). About 20 mg of the powdered sample was placed in a platinum sample holder of 8 mm dia and 10 mm length. The experiments were carried out at a uniform heating rate of 10 °C/min from room temperature to 900 °C in 1% O₂/N₂ atmosphere and at a flow rate of 50 ml/min. In addition, thermal analysis coupled with mass spectrometer were also carried out using Setaram-Sensys instrument in the temperature range from 20 °C to 820 °C in 1% O₂/N₂ atmosphere. The typical ion current curves of the different samples are shown in the figures for comparison. The purpose is to determine various components evolved during such thermal analysis in the present VPO catalysts.

The surface areas (BET-SA) and pore size distribution of the catalysts were determined on Gemini III – 2375 (Micromeritics, U.S.) by N₂-physisorption at –196 °C. Prior to the measurements, the known amount of catalyst was evacuated for 2 h at 150 °C to remove physically adsorbed water.

The X-ray diffraction (XRD) patterns were obtained on a X-ray diffractometer STADI-P (Stoe, Darmstadt, Germany) using Ni-filtered CuK_α radiation (λ = 1.5418 Å). The crystalline phases were identified by referring to the ASTM data files.

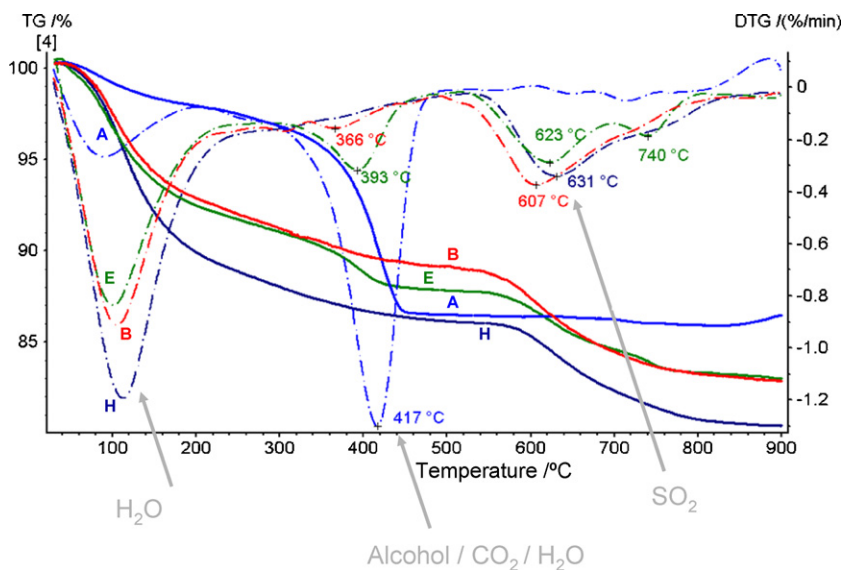


Fig. 1. TGA and DTA curves of bulk and TiO₂ supported VPO catalysts with different VPO contents (A, bulk VPO; B, 5% VPO/TiO₂; E, 20% VPO/TiO₂; H, pure TiO₂).

For the characterization of surface acidity, pyridine was adsorbed on the activated catalysts at room temperature until saturation. However, before adsorption experiments the catalysts were activated in airflow at 300 °C for 30 min to remove moisture from the samples and after such activation the samples were cooled down to room temperature. Spectra were recorded using a Bruker IFS 66 spectrometer (2 cm⁻¹ resolution, 100 scans) equipped with a heatable and evacuable IR cell with CaF₂ windows, which is connected to a gas dosing/evacuation system. For these experiments, the catalyst powder was pressed into self-supporting discs (50 mg, Ø 20 mm). Difference spectra were obtained by subtracting the spectrum of the activated catalyst at room temperature.

The X-ray photoelectron spectroscopic (XPS) measurements were done with a VG ESCALAB 220iXL unit using MgK α radiation ($E = 1253.6$ eV) at a base pressure of the UHV chamber.

2.3. Catalytic tests

Ammoxidation runs were performed in a fixed bed, tubular glass reactor at atmospheric pressure. In a typical experiment, 3 g of catalyst particles (1–1.25 mm size) mixed with equal amount of glass beads (1.7–2.0 mm) were loaded into the glass reactor (300 mm long and 12 mm i.d.) and heated in an electrical furnace. Air, NH₃ and N₂ (for dilution) supplied were commercially available gases from compressed gas cylinders. The flow rates of these gases were controlled using mass flow controllers. The 3-picoline and water were injected by means of HPLC pumps (LC-9A HPLC, Shimadzu) and were vaporized in a preheating zone provided on the top of the catalyst bed. The reaction was carried out in the range of 325–360 °C and at a mole ratio of 3-pic:H₂O:NH₃:air = 1:9:6:30 (3-pic = 10 mmol/h; cat: 3 g (4.0 ml); catalyst dilution (cat:glass beads) = 1:2 (by wt.)). Two thermocouples were positioned one at the centre of the catalyst bed to indicate reaction temperature and the other one was attached to furnace through temperature indicator cum controller to monitor the temperature of the reactor. The product stream was collected for every half-an-hour under steady state conditions and analysed by gas chromatograph (GC 17A, Shimadzu, Japan) equipped with FID module using a capillary column (FS-SE-54). The total oxidation products (CO_x) were continuously monitored by on line non-dispersive infrared analyser (Infracal 40 E, Germany).

3. Results and discussion

3.1. Elemental analysis by ICP-OES

After preparing the catalysts, the actual contents of all catalyst components were estimated using ICP-OES technique. Such ICP analysis results of various VPO/TiO₂ catalysts are shown in Table 2. The contents of vanadium, phosphorous and titanium estimated from ICP are in good agreement with those of nominal values. In addition, the contents of all these components were also checked again in the spent samples and found that they are quite comparable with those of fresh samples. This fact suggests that there is no loss of catalyst components during the course of the reaction. A slight loss of phosphorous could be noticed particularly in the spent 5% VPO/TiO₂ sample, which is however negligible.

3.2. Thermal analysis

The thermogravimetric analysis (TGA) coupled with mass spectrometer of some selected VPO/TiO₂ catalysts, bulk VPO and pure support are presented in Fig. 1(a). It is evident from Fig. 1(a) that there are three distinct stages of weight loss of catalysts. These are (i) from room temperature to 200 °C (ii) from 200 °C to 500 °C (iii) above 500 °C. The weight loss of the catalysts below 200 °C is clearly due to desorption of physically adsorbed water. It can also be seen from the figure that the bulk VPO contains small amount of physically adsorbed water (<2%) compared to pure titania and also the catalysts prepared using titania. Such low water content in bulk VPO is expected because the VPO precursor is prepared

Table 2

Estimation of V, P, Ti contents from ICP-OES in VPO/TiO₂ catalysts with different VPO loadings.

Catalyst	V		P		Ti	
	Fresh	Used	Fresh	Used	Fresh	Used
5% VPO/TiO ₂	1.6	1.4	0.9	0.7	55.4	52.6
10% VPO/TiO ₂	3.0	2.9	1.6	1.5	48.1	46.8
15% VPO/TiO ₂	4.7	4.7	2.6	2.7	45.4	45.6
20% VPO/TiO ₂	6.4	6.4	3.8	3.8	42.0	42.0
25% VPO/TiO ₂	8.6	8.9	5.3	5.3	42.6	40.0

through an organic route and hence the water content in such sample would be naturally less. On the other hand, pure TiO₂ support contains the maximum amount of water (i.e. 12–13%), which on evolution at around 120 °C exhibit an intense endothermic peak. The evolution of water at this temperature is also further confirmed by mass spectrometer, which is coupled with TG analysis (see Fig. 1(a)). In addition, the amount of water that is lost in this temperature range is decreasing with increasing VPO loading and hence the intensity of the endothermic peaks of the catalysts is also decreasing.

The second stage of weight loss occurred at around 400 °C, where the second endothermic effect can clearly be seen. This effect is undoubtedly due to the phase transformation of VHP into VPP and also partly to the evolution of alcohols trapped in the layers of VHP precursor. This is possible because benzyl alcohol and 2-butanol are used as reducing agents during preparation of catalyst samples and hence certain amounts of such alcohols are trapped in the layered structure of VHP precursor even after oven drying. The alcohols trapped in the layers have to go out during thermal treatment in the form of CO₂ as long as the oxygen is present in the calcinating atmosphere. However, O₂ concentration in the calcinating atmosphere is deliberately limited to avoid over oxidation of vanadium species to V⁺⁵ oxidation state. On the other hand, if the calcination is performed in an inert atmosphere (e.g. in N₂ or He), then the trapped alcohols during their evolution must use the lattice oxygen of VPO structure and go out again in the form of CO₂ or simply coke and poison the catalyst, as a result the catalyst gets reduced. Such situation further leads to the generation of more V⁺³ species, which in turn reduces the catalytic activity. Therefore calcinating atmosphere must be carefully chosen in order to obtain the desired phase composition. The temperature required for such transformation again depends on the VPO content of the solid. Therefore, the peak maxima during such transformation varied in the range from 366 °C (5% VPO) to 417 °C (pure VPO). Bulk VPO solid displayed the maximum weight loss at around 450 °C and then remained more or less constant. The theoretical weight loss for the transformation of VHP into VPP is around 10.5%. However, the VPOs showed slightly higher weight loss than theoretical, which is undeniably due to removal of additional trapped alcohols in the layers of precursor. As expected, pure TiO₂ did not show any such effect in this temperature range.

The third stage of weight loss is occurred at around 600 °C, which is purely due to removal of residual sulphates from the TiO₂ support. The endothermic effect due to such removal is shown only by the VPO/TiO₂ catalysts and the support but not by the bulk VPO solid due to absence of sulphates in it. The peak maxima of temperature is again depended on the content of VPO and varied in the range from 607 °C to 631 °C. The peak intensity appears to be proportional to the content of TiO₂. In other words, the higher the VPO content the lower the TiO₂ content and hence the lower the intensity of such endothermic effect. Interestingly, all the effects observed from these samples are only endothermic and no exothermic effects are noticed. It is worthwhile to mention here that the removal of H₂O, alcohols and sulphates at different stages/temperatures is also confirmed by mass spectra coupled with TG analysis. The mass spectra obtained from such analysis are shown in Fig. 2. Curves (i)–(vi) of Fig. 2 illustrate the evolution of various components such as H₂O, benzyl alcohol, ethanol, 2-butanol, CO₂ and SO₂. It can also be seen from Fig. 2 (curve-i) that the evolution of H₂O is occurring in two different stages, i.e. at <200 °C and at ca. 450 °C. As discussed above, the former one is due to removal of physically adsorbed water and the latter one is due to phase transformation from VHP to VPP. The results of TG–MS further confirm the evolution of various other components at different temperatures, which however depend upon the composition of the catalysts.

Table 3Surface areas and pore volumes of fresh and spent VPO/TiO₂ catalysts.

Catalyst	BET-SA ^a (m ² /g)	BET-SA ^b (m ² /g)	PV ^a (cm ³ /g)	PV ^b (cm ³ /g)
Pure TiO ₂ (anatase)	144	123	0.261	0.296
5% VPO/TiO ₂	133	108	0.230	0.271
10% VPO/TiO ₂	111	–	0.206	–
20% VPO/TiO ₂	92	78	0.175	0.230
50% VPO/TiO ₂	70	50	0.163	0.111
Bulk VPO	24	12	0.071	0.030

PV, pore volume.

^a Fresh catalysts.^b Spent catalysts.

3.3. BET surface areas and pore volumes

BET surface areas and pore volumes of fresh and spent VPO/TiO₂ catalysts with different VPO loadings are given in Table 3. For the sake of better comparison, the surface areas of the pure support (TiO₂) and bulk VPO are also presented in Table 3. The catalysts showed a wide range of surface areas and pore volumes depending upon the content of VPO in the samples. The specific surface areas of the supported VPO catalysts are appreciably lower than the pure support. Pure TiO₂ (anatase) has exhibited the highest surface area (144 m²/g) and pore volume (0.261 cm³/g), while the pure VPO showed the lowest (24 m²/g and 0.071 cm³/g). The surface area of pure TiO₂ is however decreased considerably after addition of VPO [29]. VPO loading had a clear impact on the surface areas and pore volumes of the samples. The surface areas are observed to decrease from 133 m²/g to 70 m²/g with increase in VPO loading from 5 wt% to 50 wt%. Spent catalysts showed considerably lower surface areas compared to their corresponding fresh samples. Such decrease in surface areas might be due to possible structural changes occurred during the course of reaction under the influence of reactant feed mixture and severe reaction conditions. Some hints on structural changes in the spent samples are also obtained from changes in pore size distribution and FTIR analysis, which are however discussed below separately.

The pore volume distribution curves of fresh VPO/TiO₂ catalysts are depicted in Fig. 3(a). The pure support has a total pore volume of 0.261 cm³/g and a total pore area of 144 m²/g. The pore size distribution of these catalysts was made by the application of N₂ adsorption method. The pure support has shown bi-modal pore volume distributions in the pore diameter range from 25 Å to 60 Å. It has shown a very narrow volume distribution at 25 Å, and a broad and prominent distribution around 60 Å; major part of the contribution to the pore volume of the sample comes from the pores located in this range [30]. However, after the addition of VPO to TiO₂ support, the narrow pore volume distribution, which originally appeared at around 25 Å in pure support is disappeared, as a result the surface area decreased. This observation points to the fact that the addition of VPO has an influence on the pore structure of resulting catalysts. All the supported VPO catalysts showed uni-modal pore volume distribution. The intensity of pore volume distribution curve is decreasing with increasing in VPO content of the solids. This result is in line with the changes in surface areas.

The pore size distribution patterns of spent VPO/TiO₂ solids are illustrated in Fig. 3(b). It is evident that the pore size distribution exhibited by the spent samples is considerably different from their corresponding fresh samples. In addition, an appreciable shift in the pore diameter towards higher pore range is also noticed irrespective of VPO content. Some pores are vanished and some new pores are also formed. This observation clearly suggests that the reaction conditions have brought about drastic changes in their pore structures and thereby surface areas and total pore volumes

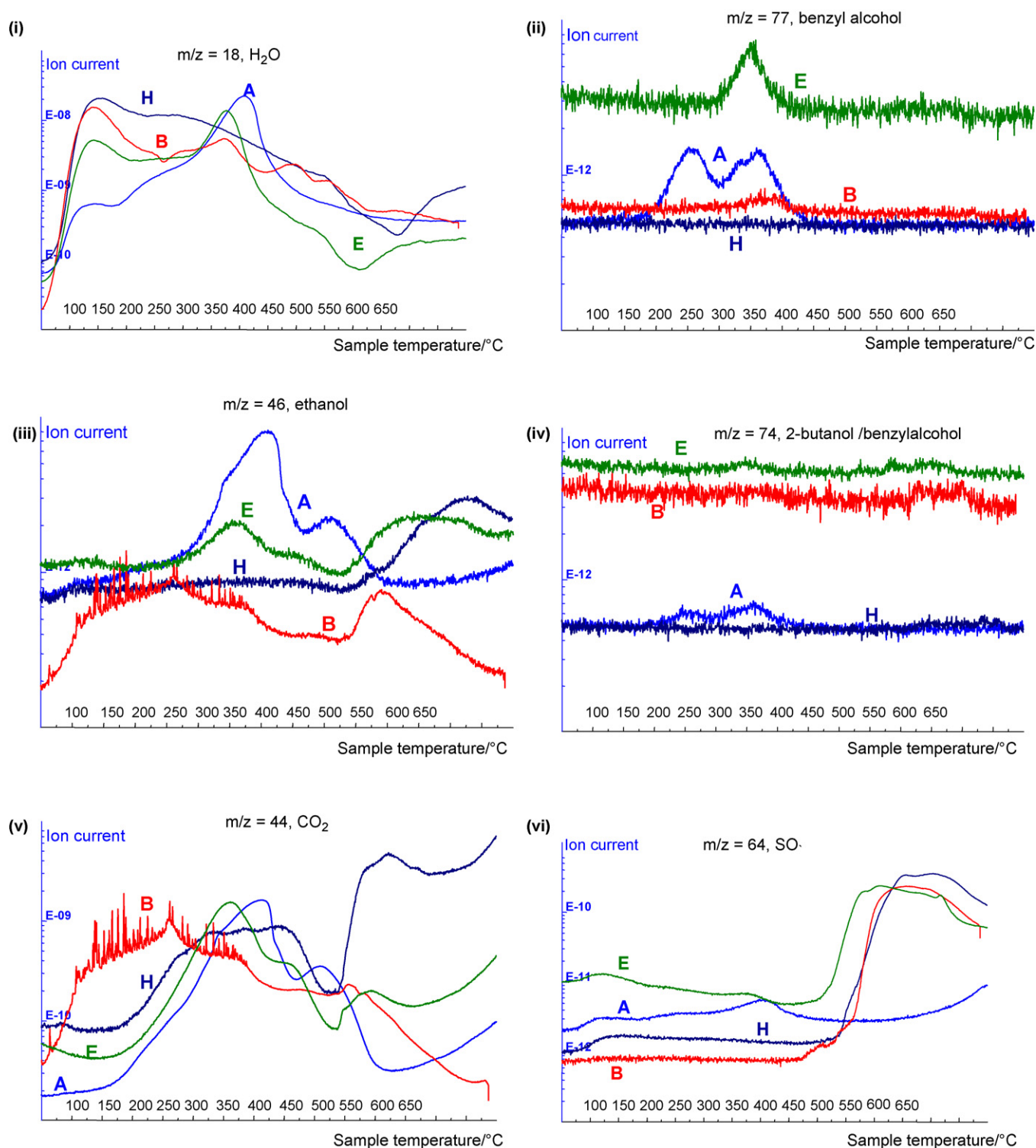


Fig. 2. Mass spectra obtained during thermal analysis over bulk and TiO₂ supported VPO catalysts (A, bulk VPO; B, 5% VPO/TiO₂; E, 20% VPO/TiO₂; H, pure TiO₂).

(see Fig. 3(b)). Interestingly, pure titania support after the catalytic tests displayed tri-modal pore volume distribution curve against bi-modal distribution in the fresh sample. The pores are located in the pore diameter range of ca. 40 Å, a narrow distribution at 85 Å and a prominent broad distribution at 155 Å. Furthermore, spent VPO/TiO₂ solids also showed similar such tri-modal distribution like support but with some variations in the intensity of pore volume distribution curves.

3.4. XRD and FTIR

XRD patterns of fresh samples confirm the formation of VPP phase in the catalysts. However, the crystalline VPP phase can only be seen in the samples with high VPO loading (>15 wt% VPO). This means the VPP phase present in the low loading VPO catalysts seems to be X-ray amorphous in nature. However, FTIR spectra of fresh solids provided good hints on the formation of VPP

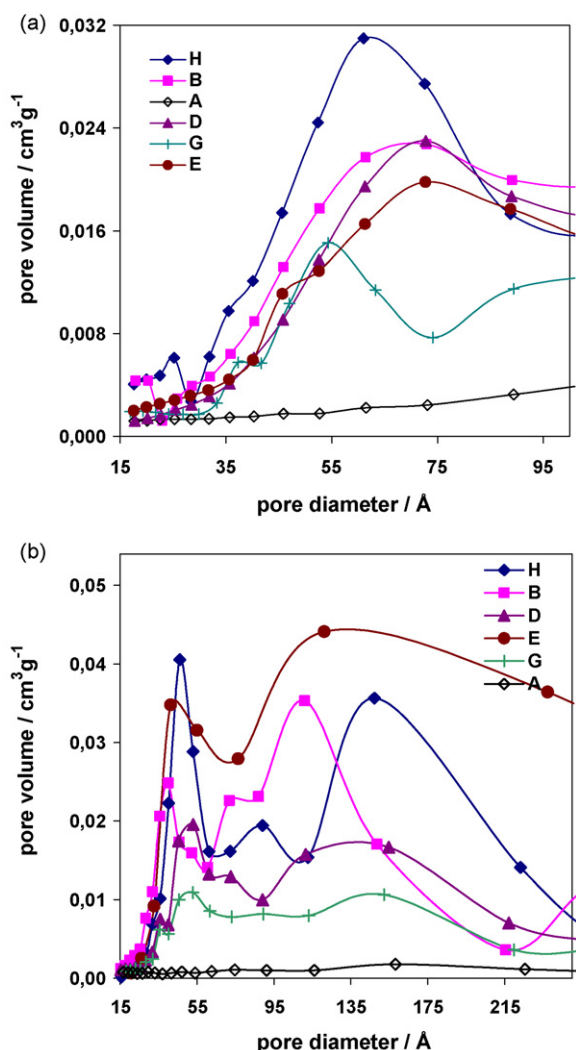


Fig. 3. (a) Pore size distribution of fresh bulk and TiO₂ supported VPO catalysts (A, bulk VPO; B, 5% VPO/TiO₂; D, 15% VPO/TiO₂; E, 20% VPO/TiO₂; G, 50% VPO/TiO₂; H, pure TiO₂). (b) Pore size distribution of spent bulk and TiO₂ supported VPO catalysts (A, bulk VPO; B, 5% VPO/TiO₂; D, 15% VPO/TiO₂; E, 20% VPO/TiO₂; G, 50% VPO/TiO₂; H, pure TiO₂).

phase even in low VPO-containing solids. No significant changes in the XRD patterns of spent samples compared to fresh ones could be noticed. The intensity of XRD reflections corresponds to VPP phase is increasing with increase in VPO contents, as expected. XRD patterns of both fresh and spent samples can be viewed from [supplementary material](#).

FTIR spectra of fresh and spent bulk and supported VPO solids are given in Fig. 4(a) and (b). FTIR spectra further confirm the formation of VPP phase in these solids. The band appeared at 634 cm⁻¹ corresponds to δ-OPO and the one at 744 cm⁻¹ is due to ν_s P-O-P vibrations. The band at 968 cm⁻¹ can be attributed to ν V⁴⁺=O species, which provides hints on the formation of VPP. Other bands appeared at 1095 cm⁻¹, 1142 cm⁻¹ and 1241 cm⁻¹ are assigned to symmetric (ν_s PO₃) and asymmetric (ν_{as} PO₃) stretching vibrations of phosphate groups (Fig. 4(a)). On the whole, FTIR gives good supporting evidence to the results obtained from XRD on the formation of active VPP phase.

There is no much difference in the FTIR spectra of the spent samples compared to fresh ones except a new band appeared at 1420 cm⁻¹ (Fig. 4(b)). This means FTIR spectra of spent samples gave further hints on the formation of NH₄-containing VPO phase

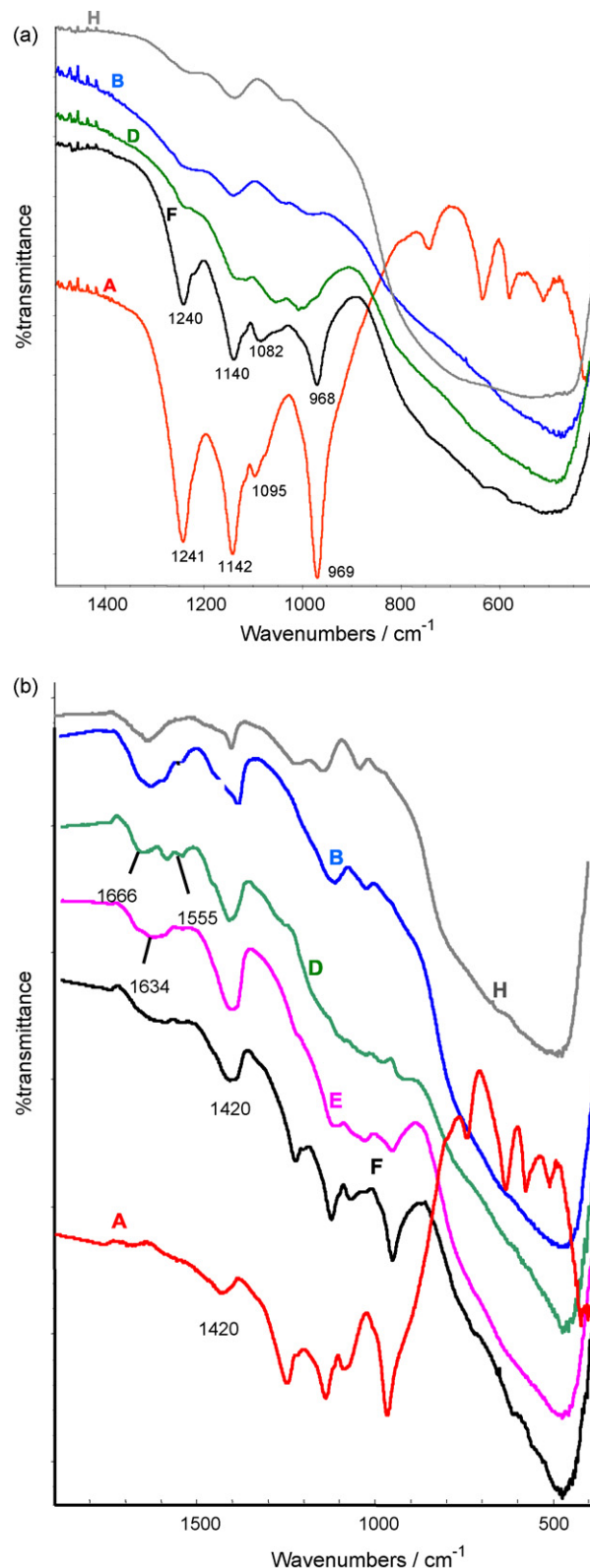


Fig. 4. (a) FTIR spectra of fresh bulk and TiO₂ supported VPO catalysts (A, bulk VPO; B, 5% VPO/TiO₂; D, 15% VPO/TiO₂; F, 25% VPO/TiO₂; H, pure TiO₂). (b) FTIR spectra of spent bulk and TiO₂ supported VPO catalysts (A, bulk VPO; B, 5% VPO/TiO₂; D, 15% VPO/TiO₂; E, 20% VPO/TiO₂; F, 25% VPO/TiO₂; H, pure TiO₂).

(i.e. more likely (NH₄)₂(VO)₃(P₂O₇)₂) in addition to the major VPP phase [31]. Formation of such phase is expected from the reaction of vanadium species with that of ammonia during the course of the reaction.

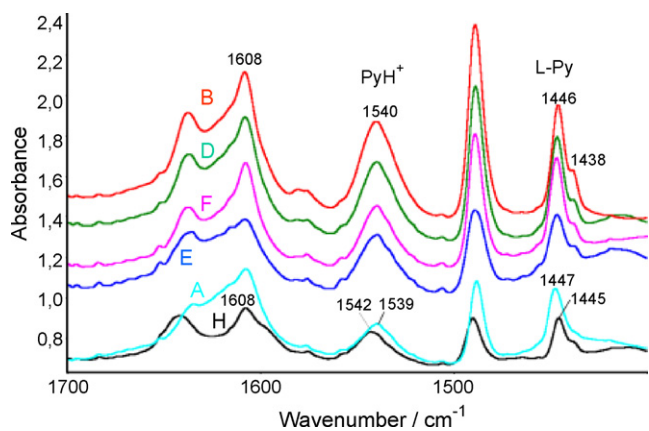


Fig. 5. Acidity measurements by FTIR pyridine adsorption at 25 °C on bulk and TiO₂ supported VPO solids (A, bulk VPO; B, 5% VPO/TiO₂; D, 15% VPO/TiO₂; E, 20% VPO/TiO₂; F, 25% VPO/TiO₂; H, pure TiO₂).

3.5. Acidity measurements by pyridine adsorption (FTIR)

For characterizing the surface acidity, pyridine used as a probe molecule was adsorbed at room temperature. Usually, the bands appeared at around 1540–1548 cm⁻¹ and 1445–1460 cm⁻¹ are characteristic bands of Brønsted (PyH⁺) and Lewis (L-Py) acid sites, respectively. Furthermore, the bands correspond to hydrogen-bonded pyridine (hb-Py) are also expected in the similar range (1440–1447 cm⁻¹ and 1590–1600 cm⁻¹) and the bands due to physically adsorbed pyridine (ph-Py) at 1439 cm⁻¹ and 1580 cm⁻¹ [e.g. [32,33]]. It should be noted that the intensity of the band is proportional to the concentration of acid sites. The FTIR spectra of present VPO/TiO₂ solids obtained after pyridine adsorption are illustrated in Fig. 5. The pyridine adsorption was carried out at two different temperatures such as room temperature and at 200 °C. At both the temperatures, the catalysts showed bands at 1446 cm⁻¹ and 1608 cm⁻¹ that correspond to Lewis sites and the other band appeared at 1540 cm⁻¹ is due to Brønsted sites. It can also be seen from the figure that all catalysts contain both Lewis and Brønsted sites in different proportions depending upon VPO content. It is also obvious from Fig. 5 that the supported VPO catalysts exhibit intense bands compared to their parent materials such as bulk VPO and pure TiO₂. This means the supported VPOs are more acidic than the parent samples. Such enhancement in the acidity characteristics

of supported catalysts designates a good and effective interaction between the support and active phase.

3.6. Pyridine desorption measurements (FTIR)

After evaluating the influence of VPO loading on the concentration of both LS and BS, further studies were focused on the desorption behaviour of adsorbed pyridine over a wide range of temperatures starting from 25 °C to 400 °C. For this purpose, three different solids such as the lowest VPO loading (5% VPO), the best VPO loading (20% VPO) and the pure TiO₂ support were selected and analysed. Comparison of pyridine desorption spectra of 5% and 20%VPO/TiO₂ and pure TiO₂ are portrayed in Fig. 6. The purpose of this study is to check the strength of acid sites as a function of temperature. All the three samples exhibited intense bands correspond to Lewis and Brønsted sites. However, the intensity of the bands is found to decrease gradually with increase in desorption temperature. It is noteworthy that these bands are still present even at 400 °C indicating their higher strength and good thermal stability. From the intensity of the bands, it can be assumed that the VPO catalyst with low loading (5%) is more acidic than the one with high VPO loading (20%). The higher acidity of low VPO catalyst seems to be arising from the support. Catalytic results showed that too much acidity enhanced total oxidation that leads to the formation of higher amounts of CO_x and hence reduces the selectivity of desired nitrile. As mentioned earlier, Fig. 6 gives good evidence for the higher acidity of pure support and also the existence of such acidic sites of support even at temperatures higher than the reaction temperature.

3.7. X-ray photoelectron spectroscopy (XPS)

XPS analysis provides information on the oxidation state of vanadium and concentration of surface elements. XP spectra of fresh VPO/TiO₂ catalysts with varying VPO loadings are given in Fig. 7(a) and (b). In Fig. 7(a), O 1s and V2p_{1/2} and V2p_{3/2} photoelectron peaks are presented while in Fig. 7(b), P2p peaks are shown. It is known from the literature [34,35], that the position of V⁺⁵ component in VPO solids lies at 518 eV while the binding energy for V⁺⁴ would be 516.9 eV [36,37]. Due to such difference in binding energy values of V⁺⁵ and V⁺⁴ components, their contributions can be well separated. On the other hand, if any V⁺³ species are present in the samples, then their contributions further shift the position of the peak to lower binding energy values and would exhibit a bigger FWHM than V⁺⁴ peak [34]. However,

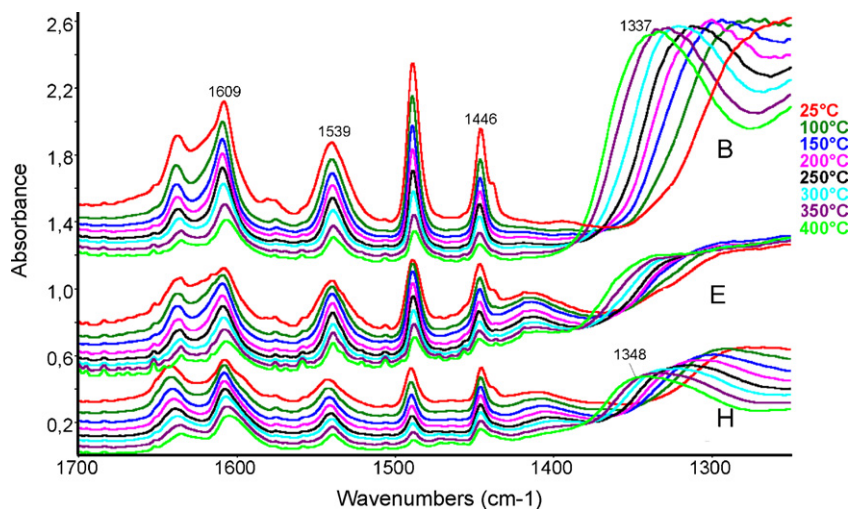


Fig. 6. Comparison of pyridine desorption spectra (FTIR) of 5% and 20% VPO/TiO₂ solids and pure TiO₂ support (B, 5% VPO/TiO₂; E, 20% VPO/TiO₂; H, pure TiO₂).

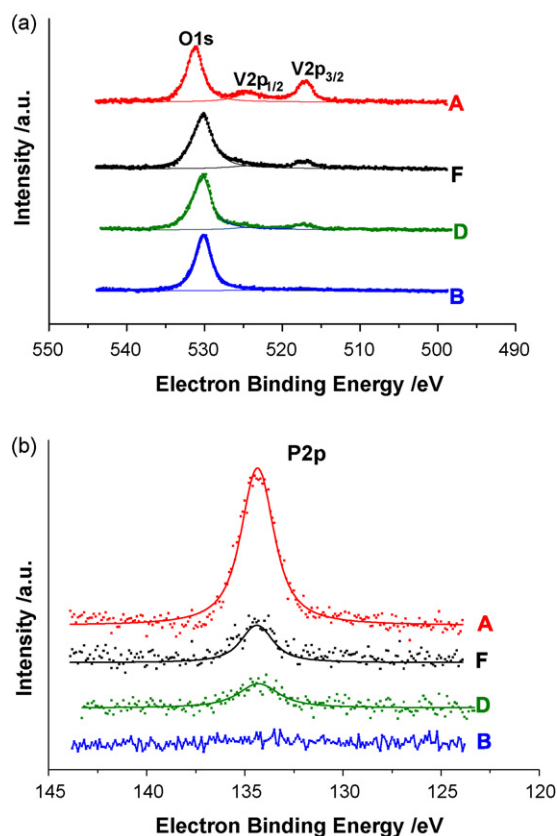


Fig. 7. (a) XP spectra for fresh VPO/TiO₂ catalysts with varying VPO loadings (showing O 1s and V 2p peaks) (A, bulk VPO; B, 5% VPO/TiO₂; D, 15% VPO/TiO₂; F, 25% VPO/TiO₂). (b) XP spectra for fresh VPO/TiO₂ catalysts with varying VPO loadings (showing P 2p peaks) (A, bulk VPO; B, 5% VPO/TiO₂; D, 15% VPO/TiO₂; F, 25% VPO/TiO₂).

one should note that V₂O₅ based catalysts exhibit somewhat lower binding energy values compared to VPO catalysts for similar oxidation states of vanadium (e.g. V⁺⁴ and V⁺⁵). Our samples showed the binding energy values at around 517.1 eV that mainly correspond to V⁺⁴ species of active VPP phase in VPO/TiO₂ solids. This value is comparable with that of the one reported above for V⁺⁴ oxidation state in literature. No significant shift in the peak position with increase in VPO loading and hence no considerable change in the vanadium valence in all the catalysts. However, the intensity of peak corresponds to V⁺⁴ species is increasing with increase in VPO content of the samples, as expected. In addition, bulk VPO solid displayed higher B.E. (531.2 eV) for O 1s peak than the supported VPOs (530.2 (±1) eV). Such difference in B.E. value between bulk and supported VPOs might be due to the presence of different nature of oxygen present in the pure VPO sample and TiO₂ supported VPOs. Fig. 7(b) shows that there is no considerable shift in the P 2p photoelectron peak position in all the samples and hence no change in binding energy values, which remained more or less constant at around 134.4 eV.

Additionally, variation of P/Ti, V/Ti and P/V surface ratios estimated from XPS in VPO/TiO₂ catalysts with different VPO loadings are given in Table 4. The P/Ti and V/Ti ratios are observed to increase with increase in VPO content of the samples. The surface P/V ratios of supported VPOs are found to be comparable with that of theoretical value (P/V = 0.95). However, an enrichment of phosphorous at the surface can clearly be seen in case of bulk VPO solid (P/V = 1.3). Enrichment of phosphorous in VPO solids is a common phenomenon and such enrichment helps stabilizing reduced vanadium species and also limits the over oxidation [e.g. [38]].

Table 4

Variation of P/Ti, V/Ti and P/V surface ratios (determined from XPS) in VPO/TiO₂ catalysts with different VPO loadings.

Catalysts	P/Ti	V/Ti	P/V
5% VPO/TiO ₂	0	0.17	–
15% VPO/TiO ₂	0.27	0.26	1.0
20% VPO/TiO ₂	0.43	0.49	0.9
Bulk VPO	–	–	1.3

3.8. Catalytic results

3.8.1. Influence of VPO loading on the catalytic performance

The influence of VPO loading on the catalytic performance of VPO/TiO₂ solids is carried out at two different temperatures such as 325 °C and 360 °C and presented in Fig. 8(a) and (b). For better comparison, the catalytic results obtained on bulk VPO sample (i.e. 100% VPO (un-supported)) are also included in both the figures. Fig. 8(a) and (b) demonstrate that the supported VPO catalysts displayed better performance than the pure VPO solid. In addition, the content of VPO has shown a strong influence on the activity and selectiv-

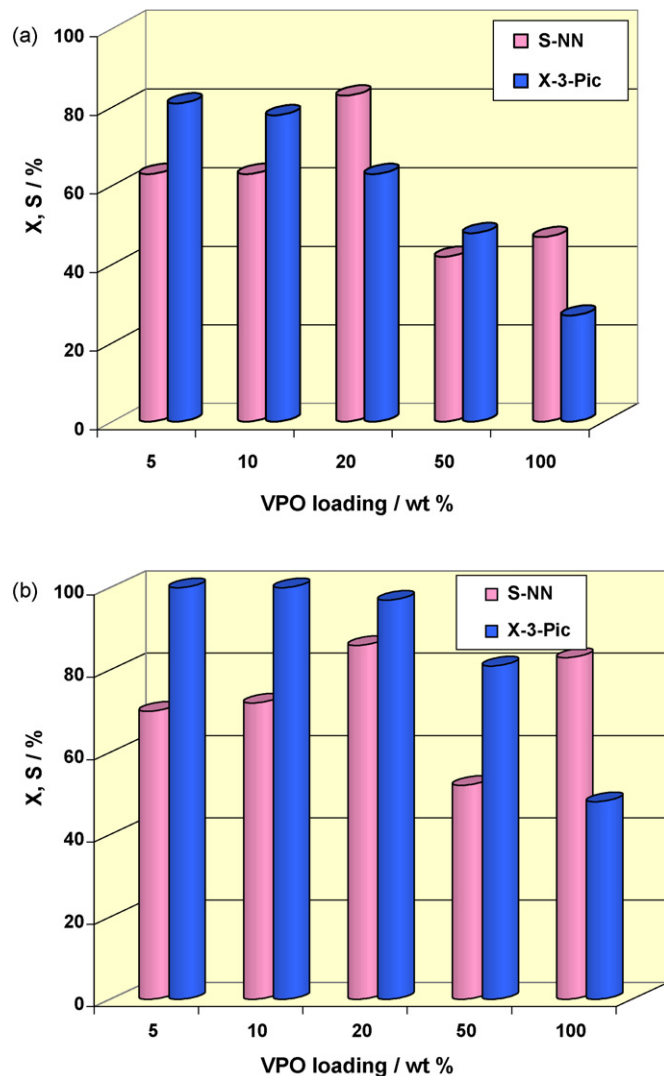


Fig. 8. (a) Catalytic performance of bulk and supported VPO solids with different VPO loadings at a temperature of 325 °C (mole ratio of 3-pic:H₂O:NH₃:air = 1:9:6:30 (3-pic = 10 mmol/h); cat: 3 g (4.0 ml); dilution (cat:glass beads) = 1:2 (by wt.)). (b) Catalytic performance of bulk and supported VPO solids with different VPO loadings at a temperature of 360 °C (mole ratio of 3-pic:H₂O:NH₃:air = 1:9:6:30 (3-pic = 10 mmol/h); cat: 3 g (4.0 ml); dilution (cat:glass beads) = 1:2 (by wt.)).

ity behaviour of the catalysts. In every case, the catalyst with the lowest VPO loading displayed the highest conversion of 3-picoline and vice versa. At low VPO contents, not only the conversion of 3-picoline is high but also the total oxidation is also considerably high, which in turn reduces the selectivity of desired product. It is evident from Fig. 8(a) that the conversion of 3-picoline decreased from 81% to 48% with increase in VPO loading from 5 wt% to 50 wt%. On the other hand, bulk VPO showed very low conversion ($X_{\text{3-pic}} = 27\%$) compared to supported catalysts. NN is the major product, while CO, CO₂ are the by-products. However, pyridine and isonicotinitrile are also observed in small amounts as side products depending upon the catalyst applied. The highest selectivity of desired product (NN) is obtained on 20 wt% VPO/TiO₂ catalyst (Fig. 8(b)). Interestingly, the same tendency is also observed when the reaction is carried out even at 360 °C. At this temperature, the catalyst with the lowest VPO loading displayed almost total conversion of 3-pic ($X = \text{ca. } 100\%$) but the selectivity of target product obtained is relatively low ($S_{\text{NN}} = 70\%$). The selectivity of NN is observed to increase from 70% to 86% with rise in VPO content from 5 wt% to 20 wt% and then decreased with further increase in VPO loading. The best optimum seems to be 20 wt% VPO, where the highest conversion of 3-picoline and yield of NN ($X = 98\%$ and $Y = 83\%$) could be obtained (Fig. 8(b)). Such increase in selectivity of NN can be attributed to the changes in acidic characteristics of the catalysts when VPO contents are changed. The correlation of acidity against activity is however discussed below in a separate section. It appears that when the VPO loading is increased beyond a certain level, the catalytic behaviour of the catalysts seems to be moving in the direction of bulk VPO and thereby reduced activity of the catalysts. At a reaction temperature of 360 °C, the bulk VPO solid gave only 48% conversion of 3-picoline with 83% selectivity of NN. Among all catalysts tested, bulk VPO showed the poorest performance in terms of yield of NN.

At low VPO loadings, the formation of total oxidation products is significantly much higher ($Y_{\text{CO}_x} > 25\%$) compared to higher VPO loadings. This is probably due to exposure of bare acidic surface of the support, which favours the total oxidation. Interestingly, the Y_{CO_x} is decreased from over 25% (5 wt% VPO) to around 10% (on 20 wt% VPO) with simultaneous increase in NN selectivity. In other words, NN selectivity is increasing at the expense of CO_x formation with rise in VPO loading to a better optimum. Moreover, the increase in VPO loading beyond 20 wt% has again caused detrimental effect on the conversion of 3-picoline, which is decreased considerably from 100% (at 5 wt%) to 48% when pure VPO is applied. This fact suggests that an increase in VPO loading beyond 20 wt% is not at all effective in improving the performance. On the whole, it can be stated that 20 wt% VPO is found to exhibit better performance in terms of both activity and selectivity compared to others.

Our results clearly showed that the performance of supported VPOs is much superior to their corresponding bulk VPO. It is also not very clear from the literature on the potential application of supported VPOs and their influence on the catalytic activity and selectivity. Some groups reported that the supported VPOs show inferior performance compared to bulk VPO while the other claim the reverse. However, such investigations are mainly devoted to study the oxidation of butane to maleic anhydride (MA) but not for ammoxidation reactions, in general. Some researchers [39–41] propose that the usage of support can result in support–oxide interaction, which in turn either hinder the formation of VPP phase or bring about some modifications in phase composition. As a result, the supported VPO catalysts might show poor performance compared to bulk VPO. In contrast, Nie et al. [42] suggest that the supported VPOs offer various potential advantages over the unsupported ones such as better heat transfer characteristics, high surface area, better mechanical strength, and controllable catalyst textures.

Overbeek et al. [39,43,44] prepared VPO catalysts using various supports and tested their performance towards oxidation of

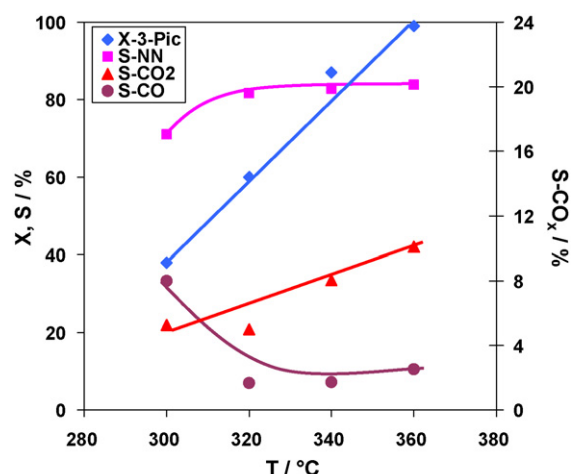


Fig. 9. Effect of temperature on the catalytic performance of 20% VPO/TiO₂ catalyst (mole ratio of 3-pic:H₂O:NH₃:air = 1:9:6:30 (3-pic = 10 mmol/h); cat: 3 g (4.0 ml); dilution (cat:glass beads) = 1:2 (by wt.)).

butane to MA. The authors claim that the use of silica enhanced the selectivity of MA but reduces the activity. On the other hand, titania improved the activity but reduces the selectivity. Such differences in the catalytic properties are assigned to the nature of interaction between active VPO phase and the support, which in turn modifies the reducibility of the catalysts. They also found a strong interaction with reducible supports such as titania and zirconia, which remarkably enhances the activity due to higher amount of active oxygen species. However, the reverse is true in case of non-reducible supports (e.g. silica), where the interaction of active phase with the support is relatively weak. In addition, Bueno et al. [45] and Li et al. [46] also report the poor performance of supported VPOs compared to bulk VPO in the oxidation of butane. On the other hand, Nie et al. [42,47] observed a significant improvement in MA selectivity when Al-MCM-41 supported VPOs are used catalysts again for butane oxidation. Our approach is completely different from all the above-mentioned reports in many ways. For instance, our method of catalyst preparation, P/V ratio of the catalyst, calcination conditions, calcination atmosphere, nature of reaction etc. are totally different and hence our results cannot be truly compared with that of literature reports where supported VPOs are used. To the best of our knowledge, articles on the application of supported VPOs for ammoxidation reactions in general and 3-picoline in particular are very rare. The superior performance of the present supported VPOs was also further confirmed by preparing similar type of VPO catalysts with the same procedure and composition and applied them for another industrially important ammoxidation reaction such as ammoxidation of 2,6-dichlorotoluene to 2,6-dichlorobenzonitrile and found again improved performance of supported VPOs compared to their parent bulk VPO. These results on the superior performance of supported VPOs are also reported in various publications [27,28,30,31,48].

3.8.2. Effect of temperature on the catalytic performance of 20%VPO/TiO₂ catalyst

Influence of reaction temperature on the activity and selectivity behaviour of VPO/TiO₂ catalysts is shown in Fig. 9. It is evident from the figure that the temperature has a highly pronounced promotional effect on the selective ammoxidation of 3-picoline over 20%VPO/TiO₂ (anatase) catalyst. The conversion of 3-picoline is observed to increase continuously from 38% to almost 100% with rise in temperature from 300 °C to 360 °C. The selectivity of NN is also increased initially and then remained more or less constant at around 80%. At the same time, the selectivity of total oxidation

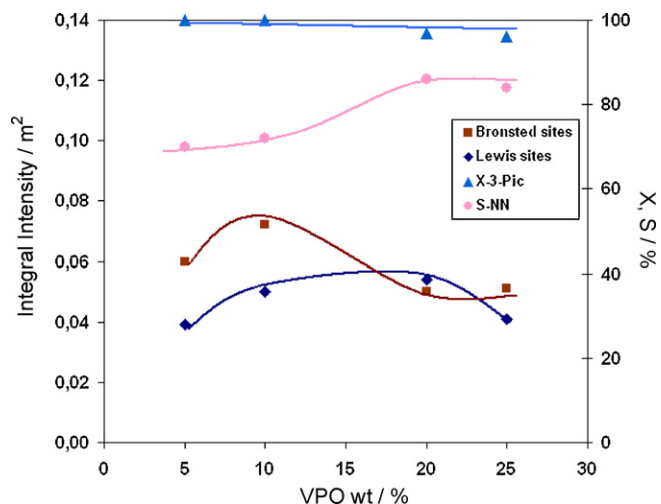


Fig. 10. Correlation of acidity per unit area with that of catalytic activity and selectivity of VPO/TiO₂ catalysts with varying VPO loadings.

products is also influenced considerably by increase in reaction temperature. The selectivity of CO decreased initially and then remained stable, while the selectivity of CO₂ has been increased continuously with rise in temperature. The maximum yield of nicotinonitrile and conversion of 3-picoline observed at 360 °C is 83% and 98%, respectively. At the same time, the yield of CO₂ is also increased from 2% to 10% with increase in temperature from 300 °C to 360 °C.

3.8.3. Correlation of acidity with that of activity over VPO/TiO₂ catalysts

The correlation of activity and selectivity behaviour of different VPO/TiO₂ solids with that of acidity characteristics is illustrated in Fig. 10. It is evident that the amount of VPO in the total catalyst has a clear influence on LS and BS integral intensity per unit surface area of the samples. The integral intensity values of BS are decreasing with increasing in VPO contents of the catalysts. On the other hand, somewhat different trend is observed concerning the integral intensity values of LS, which are increasing up to 20 wt% VPO and then decrease. It is also noteworthy that the low VPO loading catalysts contain more BS than LS. Interestingly the ratio of LS to BS is also increased up to 20 wt% VPO loading and then decreased. Alternatively, if we carefully observe the catalytic performance of these solids, the best performance is obtained over 20 wt% VPO/TiO₂ solid. Comparing these two aspects such as best performance vs acidity characteristics, it seems more probable that the acidity of the catalysts control the activity and selectivity to a greater extent. However, one should also note that too much acidity also leads to high total oxidation and at the same time too less acidity reduces the activity, as has been evidenced from the present catalytic results. Comparing these two types of acid sites (BS and LS), our results gave indications that LS appears to be more important than BS for better selectivity and thereby better yield of nitrile. If we check the concentration of these two types of acid sites on our best catalyst (20 wt% VPO), LS is slightly higher than BS. In all other samples, the integral intensity values of BS are always higher than LS. It is also noticed that wherever BS is dominating LS, the conversion is high but the selectivity is low. In contrast, when LS is dominating BS, the selectivity of desired product is high and at the same time the conversion is also maintained high as a result there is a considerable increase in the net yield of target product. It is also known that LS are necessary for initial adsorption of aromatic substrate on the catalyst surface and then forming π -complexation with the catalyst surface through π -electrons of aromatic ring fol-

lowed by H-abstraction. In conclusion, it can be said that the acidity properties are important and the concentration of both LS and BS obtained on 20% VPO solid seems to be optimum in achieving superior performance.

4. Conclusions

XRD and FTIR confirm the formation of vanadyl pyrophosphate phase in the calcined catalysts. BET surface areas and pore volumes are found to depend on the content of VPO in the total catalyst. Spent catalysts showed different pore volume distributions compared to their corresponding fresh ones. The present VPO/TiO₂ catalysts contain both BS and LS in different proportions. The acidic site distribution is also observed to depend on the concentration of VPO in the system. Pyridine desorption studies indicate that the acidic sites present in the catalysts are quite strong and remain stable even at 400 °C. VPO loading on titania has shown a strong influence on the catalytic performance. Supported VPOs exhibited superior performance compared to bulk VPO. Acidity characteristics appear to play a key role on the catalytic properties. Among different catalysts tested, 20 wt% VPO/TiO₂ has displayed the best performance in terms of higher yield of nitrile compared to others. This catalyst gave a conversion of 3-picoline close to 100% and the yield of NN is over 80%.

Acknowledgements

Thanks are due to Dr. U. Bentrup, LIKAT for FTIR measurements and Dr. J. Radnik, LIKAT for XPS measurements.

Appendix A. Supplementary data

Supplementary data associated with this article can be found, in the online version, at doi:10.1016/j.apcata.2010.07.034.

References

- [1] V.N. Kalevaru, B. David Raju, S.K. Masthan, V.V. Rao, P. Kanta Rao, R. Subrahmanian, A. Martin, *J. Mol. Catal. A: Chem.* 223 (2004) 321–328.
- [2] A. Martin, B. Lücke, *Catal. Today* 57 (2000) 61–70.
- [3] K.V. Narayana, B. David Raju, S.K. Khaja Masthan, *Catal. Lett.* 84 (2002) 27–30.
- [4] D.K. Lee, T.S. Chang, D.H. Cho, S.B. Hong, C.H. Shin, *Kor. J. Chem. Eng.* 20 (2003) 279–283.
- [5] R. Chuck, *Appl. Catal. A: Gen.* 280 (2005) 75–82.
- [6] R. Chuck, A.G. Lonza, *Proceedings of 1st Int. IUPAC Conf. on Green Sustainable Chemistry* (2006 September).
- [7] M. Sanati, A. Andersson, *J. Mol. Catal. A* 59 (1990) 233–255.
- [8] W.S. Chen, H.B. Chiany, M.D. Lee, *J. Chin. Chem. Eng.* 25 (1994) 45.
- [9] A. Andersson, S.L.T. Andersson, G. Centi, R.K. Grasselli, M. Sanati, F. Trifiro, *Appl. Catal. A: Gen.* 43 (1994) 43–57.
- [10] K.V.R. Chary, Ch. Praveen Kumar, A. Murali, A. Tripathi, A. Clearfield, *J. Mol. Catal. A: Chem.* 216 (2004) 139–146.
- [11] M. Niwa, H. Ando, H. Murakami, *J. Catal.* 49 (1977) 92–96.
- [12] K.V.R. Chary, G. Kishan, K.V. Narayana, T. Bhaskar, *J. Chem. Res. (S)* (1998) 314–315.
- [13] M.D. Allen, G.-J. Hutchings, M. Bowker, *Appl. Catal. A: Gen.* 217 (2001) 33–39.
- [14] K. Beschmann, S. Fuchs, T. Hahn, *Chem. Eng. Technol.* 70 (1998) 1436–1439.
- [15] K.V. Narayana, A. Venugopal, K.S.R. Rao, V.V. Rao, S.K. Masthan, P.K. Rao, *Appl. Catal. A: Gen.* 150 (1997) 269–278.
- [16] M. Sanati, A. Andersson, L.R. Wallenberg, B. Rebenstorf, *Appl. Catal. A: Gen.* 196 (1993) 51–72.
- [17] A. Andersson, *J. Catal.* 69 (1981) 465–474.
- [18] J.C. Otamiri, S.L.T. Andersson, A. Andersson, *Appl. Catal. A: Gen.* 65 (1990) 159–174.
- [19] K.V. Narayana, S.K. Masthan, V. Venkat Rao, P. Kanta Rao, *J. Chem. Res. (S)* (1997) 328–329.
- [20] K.V. Narayana, S.K. Masthan, V. Venkat Rao, B. David Raju, P. Kanta Rao, *Catal. Commun.* 3 (2002) 173–178.
- [21] K.V. Narayana, S.K. Masthan, V. Venkat Rao, B. David Raju, P. Kanta Rao, *Catal. Lett.* 84 (2002) 27–30.
- [22] K.M. Reddy, N. Lingaiah, P. Nagaraju, P.S. Sai Prasad, I. Suryanarayana, *Catal. Lett.* 122 (2008) 314–320.
- [23] Y. Zhang, A. Martin, H. Berndt, B. Lücke, M. Meisel, *J. Mol. Catal. A: Chem.* 118 (1997) 205–214.

- [24] G. Centi, P. Mazzoli, S. Perathoner, *Appl. Catal. A: Gen.* 165 (1997) 273–290.
- [25] M.O. Guerrero-Pérez, J.L. Rivas-Cortés, J.A. Delgado-Oyague, J.L.G. Fierro, M.A. Bañares, *Catal. Today* 139 (2008) 202–208.
- [26] M.W. Forkner, WO 2008030714 A1, Huntsman Petrochemical Corporation, USA (2008).
- [27] A. Martin, K.V. Narayana, B. Lücke, Van Deynse Dirk, M. Belmans, F. Boers, WO 03/101939 A2, Tessenderlo Chemie SA, Belgium (2003).
- [28] N. Dropka, V.N. Kalevaru, A. Martin, D. Linke, B. Lücke, *J. Catal.* 240 (2006) 8–17.
- [29] K.V. Narayana, A. Martin, U. Bentrup, B. Lücke, *J. Catal. A: Gen.* 270 (2004) 57–64.
- [30] V.N. Kalevaru, B. Luecke, A. Martin, *Catal. Today* 142 (2009) 158–164.
- [31] K.V. Narayana, A. Martin, B. Luecke, M. Belmans, F. Boers, *Z. Anorg. Allg. Chem.* 631 (2005) 25–30.
- [32] R. Buzzoni, S. Bordiga, G. Ricchiardi, C. Lamberti, A. Zecchina, G. Bellussi, *Langmuir* 12 (1996) 930.
- [33] G. Busca, *Phys. Chem. Chem. Phys.* 1 (1999) 723.
- [34] Y. Suchorski, B. Munder, S. Becker, L. Rihko-Struckmann, K. Sundmacher, H. Weiss, *Appl. Surf. Sci.* 253 (2007) 5904–5909.
- [35] S. Albonetti, F. Cavani, F. Trifiro, P. Venturoli, G. Calestani, M. Lopez Granados, J.L. Fierro, *J. Catal.* 160 (1996) 52.
- [36] Y. Suchorski, L. Rihko-Struckmann, F. Klose, Y. Ye, M. Alandjiyska, K. Sundmacher, H. Weiss, *Appl. Surf. Sci.* 249 (2005) 231.
- [37] L. Rihko-Struckmann, Y. Ye, L. Chalakov, Y. Suchorski, H. Weiss, K. Sundmacher, *Catal. Lett.* 109 (2005) 89.
- [38] J. Guan, H. Xu, S. Jing, S. Wu, Y. Ma, Y. Shao, Q. Kan, *Catal. Commun.* 10 (2008) 276–280.
- [39] R.A. Overbeek, A.R.C.J. Pikelharing, A.J. van Dillen, J.W. Geus, *Appl. Catal. A: Gen.* 135 (1996) 231–248.
- [40] N.T. Do, M. Baerns, *Appl. Catal.* 45 (1988) 1–7.
- [41] N.T. Do, M. Baerns, *Appl. Catal.* 45 (1988) 9–26.
- [42] W.Y. Nie, X.S. Wang, W.J. Ji, Q.J. Yan, Y. Chen, C.T. Au, *Catal. Lett.* 76 (2001) 201–206.
- [43] R.A. Overbeek, P.R. Warringa, M.J.D. Crombag, L.M. Visser, A.J. van Dillen, J.W. Geus, *Appl. Catal. A* 135 (1996) 209–230.
- [44] R.A. Overbeek, E.J. Bosma, D.W.H. de Blauw, A.J. van Dillen, H.G. Bruil, J.W. Geus, *Appl. Catal. A* 163 (1997) 19–144.
- [45] J.M.C. Bueno, G.K. Bethke, M.C. Kung, H.H. Kung, *Catal. Today* 43 (1998) 101–110.
- [46] X.-K. Li, W.-J. Ji, J. Zhao, Z.-B. Zhing, C.-T. Au, *J. Catal.* 238 (2006) 232–241.
- [47] W.Y. Nie, Z.Y. Wang, W.J. Ji, Y. Chen, C.T. Au, *Appl. Catal. A: Gen.* 244 (2003) 265–272.
- [48] A. Martin, V.N. Kalevaru, Q. Smejkal, *Catal. Today* (in press) doi:10.1016/j.cattod.2010.01.037.